energy charged-particle induced fission. At 340-Mev protons, the cross sections of masses 66 and 155 are equal. Therefore, the fissioning nucleus giving rise to $A=66$ must have had enough excitation energy to lose many nucleons either before or after scission. The sum of the fission-fragment masses must be not greater than 221, and probably at least two mass units less.

On the other hand, those nuclides on the heavy-mass wing are seen in low-energy fission. The fission yield of Eu^{156} varies but slightly (from 0.06 to 0.09%) over the entire energy range of charged particles used. The slopes of all fission-product distributions in the region $A \geq 150$ (Figs. 1 and 2) are very nearly identical at all charged-particle energies used in this work.

IV. ACKNOWLEDGMENTS

We wish to thank Mrs. Nancy Lee and Mrs. Joyce Gross for technical assistance; Mr. J. T. Vale and the crew of the 184-in. cyclotron, and the late Mr. G. B. Rossi and the crew of the 60-in. cyclotron for their cooperation in making the bombardments possible.

PHYSICAL REVIEW VOLUME 111, NUMBER 3 AUGUST 1, 1958

Scattering of Protons in a Spin-Orbit Potential*

G. W. ERICKSON AND W. B. CHESTON
School of Physics, University of Minnesota, Minneapolis, Minnesota
(Received March 31, 1958)

An approximation method is described for treating spin-orbit potentials in the optical model. The method is essentially a perturbation expansion using exact scattering amplitudes for a central optical potential as the unperturbed scattering amplitudes. The method is compared to an exact calculation and its usefulness in the medium-energy region demonstrated. The effects of a spin-orbit term on the differential cross section and the spin polarization distribution are investigated as a function of the parameters involved in the medium-energy region. The polarization is shown to be approximately independent of the shape of the form factor of the spin-orbit term in this energy region. The reaction cross section is insensitive to the inclusion of a spin-orbit term of reasonable depth.

INTRODUCTION

EXTENSIVE analysis has been carried out in the last few years on the scattering of 10–95 Mev protons, using a central optical model potential.[1] This analysis has been moderately successful in that it has been possible to obtain angular distributions of elastically scattered protons in reasonable agreement with the experimental data although variance of the predicted angular distributions with the data at large angles and for light target nuclei is a persistent feature of the analysis. The central optical model has also been successful in understanding the total reaction cross section for medium-energy protons although the experimental data are quite meager.[2] Neither for the elastic scattering cross sections nor for the reaction cross sections is it possible to obtain a unique set of optical model parameters (i.e., depths of the real and imaginary parts of the potential well, V and W; the falloff parameter, a; the "radius" parameter, R) which fit the experimental data. It has been conjectured by many authors that the disagreements with experiment and the ambiguity of the results of the optical model analysis using a central potential would be removed by the inclusion of spin-orbit terms in the potential. The inclusion of spin-orbit terms for bound states of protons in the nuclear shell model has, for the heavy elements, yielded real well depths in approximate agreement with those obtained by optical model analysis of scattered protons, but the falloff or surface thickness parameters so obtained are not in good agreement.[3] The analysis of scattering of 300-Mev protons using a spin-orbit potential has been recently reported.[4] Although the experimental data relevant to the properties of a proton-nucleus spin-orbit potential for intermediate-energy protons are meager except for angular distributions of elastically scattered protons, it was decided to undertake an exploration of the effects produced by a spin-orbit potential.

This study was intended to serve a variety of purposes. The examination of the effect of the spin-orbit potential on the features of the angular distribution of elastically scattered protons was undertaken

* Sponsored in part by the joint program of the Office of Naval Research and the U. S. Atomic Energy Commission. The initial stages of the research were carried out under a grant from the General Research Fund of the Graduate School, University of Minnesota. A preliminary report of this work was presented at the 1957 Thanksgiving meeting of the American Physical Society [G. W. Erickson and W. B. Cheston, Bull. Am. Phys. Soc. Ser. II, 2, 354 (1957)].

[1] Glassgold, Cheston, Stein, Schuldt, and Erickson, Phys. Rev. **106**, 1207 (1957); Melkanoff, Moszkowski, Nodvik, and Saxon, Phys. Rev. **101**, 507 (1957); A. E. Glassgold and P. J. Kellogg, Phys. Rev. **107**, 1372 (1957); see also other references included in the above papers.

[2] J. T. Gooding, Bull. Am. Phys. Soc. Ser. II, **2**, 350 (1957).

[3] Ross, Mark, and Lawson, Phys. Rev. **102**, 1613 (1956).

[4] Bjorklund, Blandford, and Fernbach, Phys. Rev. **108**, 795 (1957).

to understand whether better agreement with the experimental data at large scattering angles and light target nuclei could be obtained. In addition, the features of the polarization of the elastically scattered protons as a function of the parameters of the optical model were to be explored. As was the case in the original studies with the central optical model, exact phase shifts were to be obtained using a program prepared for the Univac Scientific Computer (E.R.A. 1103). However, during the preparation of a new code suitable for including spin-orbit potentials, an approximation method for calculating the relevant phase shifts was developed. This communication includes a description of this approximation method, the comparison of results obtained with the approximation and exact calculations, and the results of the approximation method as applied to a calculation of the angular distribution of elastically scattered protons and the resultant proton polarization as a function of the optical model parameters.

APPROXIMATION METHOD

The interaction of a nonrelativistic proton with a nucleus will be represented by a phenomenological optical model potential of the form

$$V(\mathbf{r},\boldsymbol{\sigma})=V_C(r)+(V+iW)f(r)+(v+iw)h(r)\boldsymbol{\sigma}\cdot\mathbf{L}, \quad (1)$$

where $V_C(r)$ is the electrostatic potential; V and W are the real and imaginary parts of the central part of the optical model potential; v and w are the real and imaginary parts of the spin-orbit part of the potential; $f(r)$ and $h(r)$ are the form factors of the central and spin-orbit parts of the potential (for the work reported here, the form factors for the real and imaginary parts of, for example, the central potential are chosen to be the same).[5] The elastic scattering amplitude for a proton in a potential of the form of Eq. (1) can be decomposed into two incoherent parts, the "non-spin-flip" amplitude $f(\theta)$ and the "spin-flip" amplitude $g(\theta)$, where

$$f(\theta)=\sum_L(2L+1)^{-1}\{(L+1)a_L^{+}+La_L^{-}\}P_L(\cos\theta), \quad (2)$$

$$g(\theta)=-\sum_L(2L+1)^{-1}\{a_L^{+}-a_L^{-}\}\frac{d}{d\theta}P_L(\cos\theta). \quad (3)$$

The potential of Eq. (1) has no off-diagonal elements in the (J, L, M_J) representation. The effective central potential seen by a proton in a state $J^{+}=L+\frac{1}{2}$ is

$$V_L^{+}=V_C(r)+(V+iW)f(r)+L(v+iw)h(r), \quad (4a)$$

whereas a proton in a state $J^{-}=L-\frac{1}{2}$ sees an effective central potential of the form

$$V_L^{-}=V_C(r)+(V+iW)f(r)-(L+1)(v+iw)h(r). \quad (4b)$$

The superscripts to the a coefficients of Eqs. (2) and (3) refer to the two possible J states of a proton with orbital angular momentum L in an obvious manner. For an unpolarized beam of incident protons, the differential scattering cross section $\sigma(\theta)$ is given by

$$\sigma(\theta)=|f(\theta)|^2+|g(\theta)|^2, \quad (5)$$

and the angular distribution of the spin polarization $\Pi(\theta)$ is

$$\Pi(\theta)=i[f^*(\theta)g(\theta)-f(\theta)g^*(\theta)]\sigma^{-1}(\theta), \quad (6)$$

where the polarization axis is defined by the vector $\mathbf{k}_{\text{inc}}\times\mathbf{k}_{\text{scat}}$. The derivations of Eqs. (5) and (6) are straightforward.[6]

The a coefficients for the scattering amplitudes are explicitly functions of the depths of the real and imaginary parts of the central and spin-orbit parts of the optical model potential. The approximation method considered in the intermediate energy region consists in expanding the a coefficients in Maclaurin series in $Z^{+}=L(v+iw)$ or $Z^{-}=-(L+1)(v+iw)$:

$$a_L^{+}=\sum_n\left(\frac{\partial}{\partial Z^{+}}\right)^n a_L\Big|_{Z^{+}=0}\frac{1}{n!}(Z^{+})^n, \quad (7a)$$

$$a_L^{-}=\sum_n\left(\frac{\partial}{\partial Z^{-}}\right)^n a_L\Big|_{Z^{-}=0}\frac{1}{n!}(Z^{-})^n, \quad (7b)$$

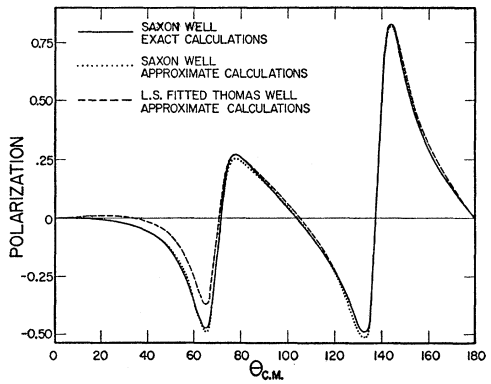

FIG. 1. The polarization distribution for 14-Mev protons scattered from carbon. The parameters of the central part of the well are $V=-50$ Mev, $W=-8.5$ Mev, $R=2.845\times10^{-13}$ cm, $a=0.5\times10^{-13}$ cm. The solid curve was calculated exactly with spin-orbit parameters $v=-1$ Mev, $w=0$, and a Saxon form factor. The dotted curve is the result using the approximation method. The rms difference between the solid and dotted curves is approximately 3%. The dashed curve is the polarization distribution calculated approximately with a Thomas spin-orbit form factor; the parameters for the Thomas spin-orbit well were chosen by requiring the polarization distribution to approximate in a least-squares manner that obtained with the Saxon spin-orbit form factor yielding $v_T\approx-310$ Mev, $w_T\approx0$. The root-mean-square difference in the dotted and dashed curves is approximately 8%.

[5] This form for the spin-orbit potential is somewhat unrealistic. For reasonable values W and w (say, -8 Mev and -1 Mev, respectively), the transmission coefficients for the J^{-} states for $L\gtrsim10$ become negative. There is little guidance from nuclear dynamics as to how L dependence should be inserted into w to insure a realistic cutoff for w in order to obviate this difficulty. We are grateful to Dr. Charles E. Porter for discussions of this point.

[6] See, for example, H. Bethe and P. Morrison, *Elementary Nuclear Theory* (John Wiley and Sons, Inc., New York, 1956), second edition, Chap. XVII.

TABLE I. The root-mean-square values of quantities salient to the approximate calculation of $\Pi(\theta)$ and $\sigma(\theta)$. The symbol

$$\text{rms}(x/x_0) \text{ means } [(1/n)\Sigma_n |x(\theta_n)/f(\theta_n)|^2]^{\frac{1}{2}}.$$

The other symbols employed are defined in the body of this communication. The case studied is 14-Mev protons on carbon with potential parameters $V=-50$ Mev; $W=-8.5$ Mev; $v=-1$ Mev; $w=0$, $R=1.243\,A^{\frac{1}{3}}\times10^{-13}$ cm, $a=0.5\times10^{-13}$ cm, $h(r)=f(r)$.

x	z^2f_2	zg_1	z^2g_2	$g-g_1z$	$g-(g_1z+g_2z^2)$
rms (x/x_0)	0.020	0.279	0.011	0.015	0.010

where a_L is the a coefficient for a proton moving in an equivalent central well.

Such an expansion would become useful whenever, for example, $|Z/(V+iW)|<1$. Although values of v and w for protons in the 10–95 Mev region are unknown, we shall show that reasonable values of v and w inferred from the bound state and 300-Mev analyses[3,4] suggest the applicability of the above expansion in the medium-energy region. Considering the leading terms in the expansion in $z=v+iw$ of $g(\theta)$ and $f(\theta)$, we find

$$f(\theta)=f_0(\theta)+f_2(\theta)z^2+\cdots, \tag{8a}$$

$$g(\theta)=g_1(\theta)z+g_2(\theta)z^2+\cdots, \tag{8b}$$

where

$$f_0(\theta)=f(\theta)\,|_{z=0},$$

$$f_2(\theta)=\sum_L \tfrac{1}{2}L(L+1)\frac{\partial^2}{\partial z^2}a_L\bigg|_{z=0} P_L(\cos\theta),$$

$$g_1(\theta)=-\frac{\partial}{\partial\theta}\frac{\partial}{\partial z}f(\theta)\bigg|_{z=0},$$

$$g_2(\theta)=\tfrac{1}{2}\frac{\partial}{\partial\theta}\frac{\partial^2}{\partial z^2}f(\theta)\bigg|_{z=0}.$$

Thus, treating the spin-orbit part of the optical model potential as small compared to the central part, we see that the first order effect upon $f(\theta)$ vanishes whereas the spin-flip scattering amplitude $g(\theta)$ can be calculated to second order in z from a knowledge of $f(\theta)$ for a family of central potentials whose depth parameters differ slightly from one another.

The method outlined above has been applied to the scattering of 14-Mev protons from C and has been tested against an exact calculation.[7] For this comparison, the form factors for the central and spin-orbit parts of the nuclear potential were both chosen to be of the Eckart or Saxon form, namely:

$$f(r)=h(r)=\left[1+\exp\left(\frac{1}{a}(r-R)\right)\right]^{-1}. \tag{9}$$

The parameters of the potential were chosen to be $V=-50$ Mev; $W=-8.5$ Mev; $v=-1$ Mev; $w=0$; $R=1.243A^{\frac{1}{3}}\times10^{-13}$ cm; $a=0.5\times10^{-13}$ cm. Since the angular distribution of the spin polarization can be written in terms of g/f alone, i.e.,

$$\Pi(\theta)=(1+|g/f|^2)^{-1}2\,\text{Re}(ig/f), \tag{10}$$

and the cross section, in this approximation, as

$$\sigma(\theta)=|f|^2\{|f_0/f|^2+[2\,\text{Re}(f_0/f)^*(f_2/f)+|g_1/f|^2]z^2+\cdots\},$$

the quantities of salient interest in the comparison were chosen to be the root-mean-square value of the following quantities: $z^2f_2(\theta)/f(\theta)$, $zg_1(\theta)/f(\theta)$, $z^2g_2(\theta)/f(\theta)$, $[g(\theta)-zg_1(\theta)]/f(\theta)$, $[g(\theta)-zg_1(\theta)-z^2g_2(\theta)]/f(\theta)$, where $f(\theta)$ and $g(\theta)$ are the non-spin-flip and spin-flip amplitudes of the exact calculation. These rms values are listed in Table I. It is quite evident from these rms values that the approximation method yields results for this energy and in this region of parameter space which are exceedingly close to those of the exact calculation. This is exhibited more strikingly in Fig. 1, where the spin polarization distribution $\Pi(\theta)$ is calculated with both the exact (solid curve) and the approximate (dotted curve) methods; these two polarization distributions are experimentally indistinguishable. Another comparison of the exact and approximate methods is shown in Fig. 2, where the exact and approximate spin-flip amplitudes are plotted in the complex plane. Although this plot is a more accurate comparison of the two methods, the physically measurable quantities such as the polarization distribution provide a more realistic comparison.

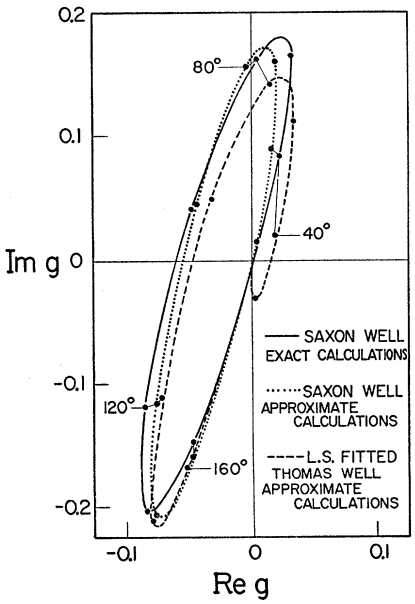

FIG. 2. The spin-flip amplitude in the complex plane for 14-Mev protons scattered from carbon. The well parameters and curve labeling is the same as for Fig. 1. Points on the curves of common scattering angle are connected.

[7] The authors are indebted to Professor A. E. Glassgold for providing them with the results of this exact calculation.

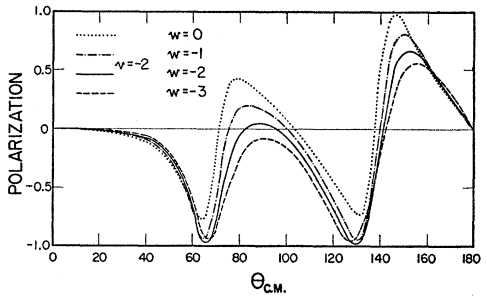

FIG. 3. The variation of the polarization distribution with w for fixed nonzero v. The case is 14-Mev protons on carbon; the central well parameters are those of Fig. 1. The Saxon form for the spin-orbit term is used; the spin-orbit well depths are in Mev.

The polarization distribution up to third order in z can be written by using Eqs. (8) and (10):

$$\Pi(\theta)=2\,\mathrm{Re}\{iz(g_1/f_0)+iz^2(g_2/f_0)\}$$
$$-2\,\mathrm{Re}\{iz(g_1/f_0)\,|g_1z/f_0|^2+iz^3[g_1f_2/f_0^2-g_3/f_0]\}.$$

The leading spin-orbit correction f_2 to $f(\theta)$ does not appear until third order in z and is a small contribution to Π compared to g_1 and g_2. If we keep terms up to order z^2 in $\Pi(\theta)$ and make use of the relations of Eq. (8), we discover that:

$$\Pi(\theta)=2i\,\mathrm{Im}\left[\Gamma\frac{\partial}{\partial\theta}\ln f\right],$$

where

$$\Gamma\equiv\left[\exp\left\{-z\left(\frac{\partial}{\partial z}\right)_{z=0}\right\}-1\right].$$

If Γ is a real operator (i.e., $w=0$), then:

$$\Pi(\theta)=-2\Gamma\frac{\partial}{\partial\theta}\phi,$$

where ϕ is the phase of the non-spin-flip scattering amplitude, i.e., $\phi=\arctan(\mathrm{Im}f/\mathrm{Re}f)$.

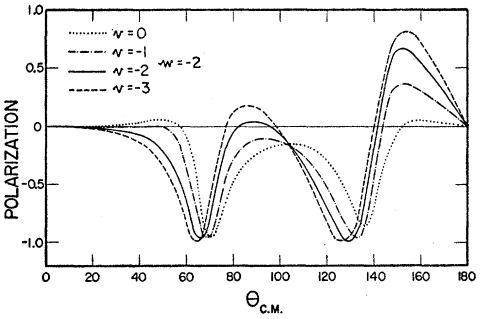

FIG. 4. The variation of the polarization distribution with v for fixed nonzero w. The case is 14-Mev protons on carbon; the central-well parameters are those of Fig. 1. The Saxon form for the spin-orbit term is used; the spin-orbit well depths are in Mev.

APPLICATION OF APPROXIMATION METHOD

The approximation method described above was applied in several studies of the effect of a spin-orbit term on various features of elastic scattering phenomena. These studies were confined mostly to the 14-Mev p-C case, where the method had been tested against an exact calculation. However, qualitatively the conclusions are expected to hold throughout the periodic table in the medium energy range.

The radial form factor for the spin-orbit term in nuclear physics has little *a priori* justification. It is

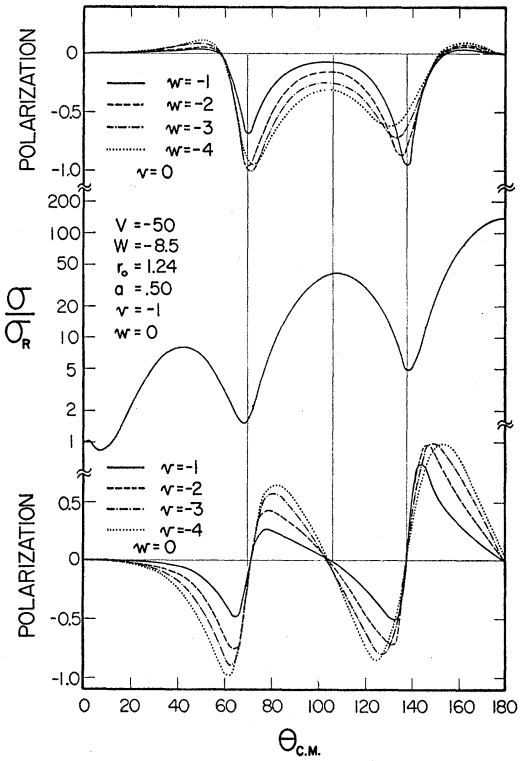

FIG. 5. The variation of the polarization distribution with w for $v=0$ (top curves) and with v for $w=0$ (bottom curves). Also included is the differential scattering cross section in ratio to Rutherford cross section. The well-depth parameters are in Mev and the length parameters in 10^{-13} cm. The case is 14-Mev protons on carbon. It is interesting to note the approximate relation when $w=0$, the polarization is zero whenever σ/σ_R is at an extremum; this feature does not persist in the region where Coulomb effects dominate.

conventional in shell-model and scattering calculations to use the so-called Thomas form[8]:

$$h_T(r)=-\left(\frac{\hbar}{2Mc}\right)^2\frac{1}{r}\frac{d}{dr}f(r). \qquad (11)$$

[8] The M in Eq. (11) refers to the nucleon mass. In the work of Bjorklund *et al.* (see reference 4), μ, the pion mass, appears in place of $2M$. The sign of $h_T(r)$ has been chosen as follows: with $v<0$, states of J^+ lie lower than states of J^-.

An attempt was made to ascertain in what sense the polarization distribution was sensitive to the functional form of $h(r)$. Figure 1 exhibits the polarization predicted with two different choices of $h(r)$, i.e., $h(r)=f(r)$, a Saxon form, and $h(r)=h_T(r)$, the Thomas form. The polarization for 14-Mev protons on carbon was found to be essentially shape independent. This shape independence was exhibited in the following manner: the results with a Thomas form for $h(r)$ using different values of (v,w) were required to approximate as well as possible in a least-squares sense over the entire angular range the results for a Saxon form for $h(r)$ with $v=-1$ Mev and $w=0$. Figure 1 shows that the polarization is only sensitive to the form of $h(r)$ in the forward direction. This demonstration of shape independence

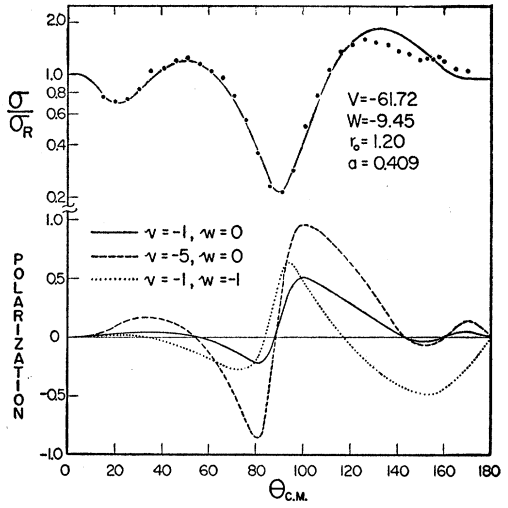

FIG. 6. The lower set of curves are typical polarization distributions for 10-Mev protons on argon. The upper curve is the angular distribution in ratio to Rutherford calculated by Glassgold *et al.* (see reference 1) using a central potential. The spin-orbit well is of the Saxon form. All depth parameters are in Mev and length parameters in 10^{-13} cm.

is shown also in Fig. 2 where the spin-flip amplitudes in the complex g plane are compared. The equivalence of the two forms may be expressed at 14 Mev as

$$v_T \simeq 0.31 \times 10^3 v_S, \tag{12}$$

where v_T and v_S are the depths of the real parts of the spin-orbit potential for Thomas and Saxon form factors, respectively. The results to be discussed below for $v_S=-1$ Mev can be thought of as approximate results with $v_T \approx -300$ Mev. A value of $v_S=-1$ Mev corresponds, therefore, to a spin-orbit well approximately $1\frac{1}{2}$ times *larger* than that used by Bjorklund *et al.*[4] in the analysis of the scattering of 300-Mev protons and is approximately 3–5 times *smaller* than that employed by Ross *et al.*[3] in shell-model calculations. It therefore

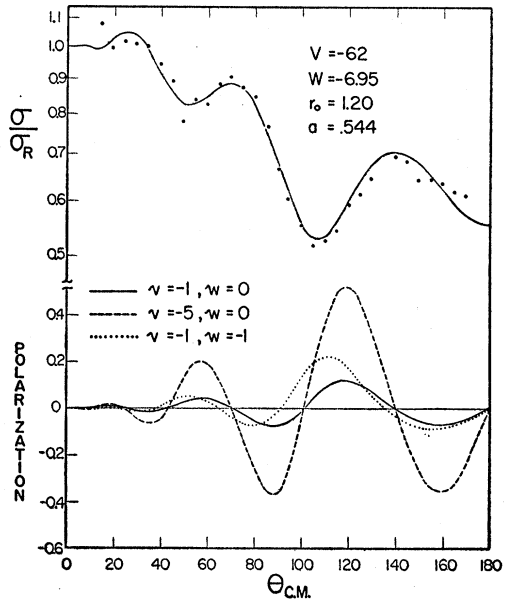

FIG. 7. The lower set of curves are typical polarization distributions for 10-Mev protons on tin. The upper curve is the angular distribution in ratio to Rutherford calculated by Glassgold *et al.* (see reference 1) using a central potential. The spin-orbit well is of the Saxon form. All depth parameters are in Mev and length parameters in 10^{-13} cm.

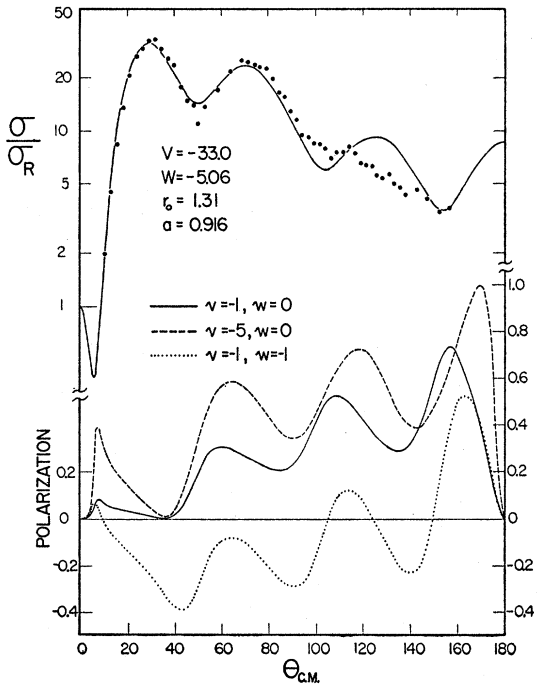

FIG. 8. The lower set of curves are typical polarization distributions for 40-Mev protons on carbon. The upper curve is the angular distribution in ratio to Rutherford by A. E. Glassgold and P. J. Kellogg [Phys. Rev. **109**, 1291 (1958)] using a central potential. The spin-orbit well is of the Saxon form. All depth parameters are in Mev and length parameters in 10^{-13} cm.

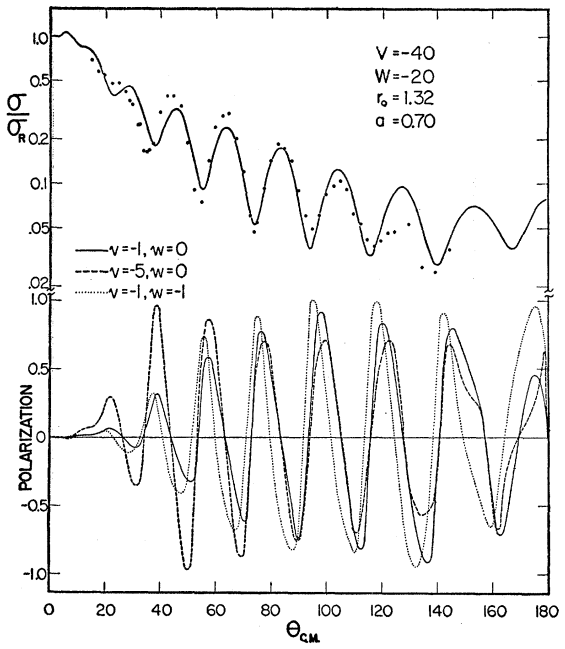

FIG. 9. The lower set of curves are typical polarization distributions for 40-Mev protons on lead. The upper curve is the angular distribution in ratio to Rutherford by A. E. Glassgold and P. J. Kellogg [Phys. Rev. **109**, 1291 (1958)] using a central potential. The spin-orbit well is of the Saxon form. All depth parameters are in Mev and length parameters in 10^{-13} cm.

seems a reasonable value for the energy range considered here.[9]

Polarization calculations were performed to ascertain the dependence of $\Pi(\theta)$ upon v and w. In Figs. 3 and 4, $\Pi(\theta)$ is displayed for fixed $v_S=-2$ Mev and w_S varied from 0 to -3 Mev (Fig. 3) and for fixed $w_S=-2$ Mev and v_S varied from 0 to -3 Mev (Fig. 4). It is quite evident, at least for proton energies of 10–20 Mev and

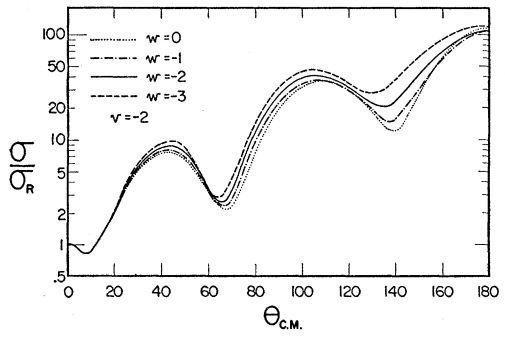

FIG. 10. The effect of changes in the imaginary part of the spin-orbit potential on the angular distribution of protons scattered from carbon at 14 Mev. The parameters of the central part of the well are those of Fig. 1. The form factor for the spin-orbit term is of the Saxon type; the well depths are in Mev.

[9] Spin-orbit wells of the Thomas form with a depth of about -600 Mev have been used in exact calculations at 40 Mev by the Livermore group. [F. Bjorklund (private communication to N. Hintz).]

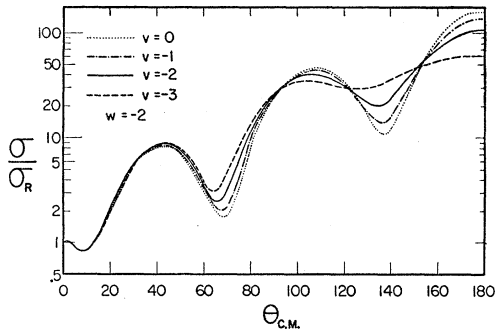

FIG. 11. The effect of changes in the real part of the spin-orbit potential on the angular distribution of protons scattered from carbon at 14 Mev. The parameters of the central part of the well are those of Fig. 1. The form factor for the spin-orbit term is of the Saxon type; the well depths are in Mev.

light target nuclei, that $\Pi(\theta)$ is sensitive to large changes in $-v$ and $-w$. Figure 5 contains the results of similar calculations for sets of runs in which ($v=0$, $w\neq 0$) and ($w=0$, $v\neq 0$). Figures 6–9 display the polarizations produced by various spin orbit wells for the following reactions: p-A and p-Sn at 10 Mev, and p-C and p-Pb at 40 Mev.

Spin-orbit wells of moderate depth produce sizable polarizations in the medium-energy region. The polarization distribution varies rapidly with energy, however. As an empirical guide for ascertaining the regions of large polarization, it has been noted that polarizations are largest whenever the differential cross section (in ratio to the Rutherford cross section) has a point of inflection; $\Pi(\theta)\approx 0$ whenever this quantity has attained an extremum. (See Fig. 5.) We have been unable to construct an analytical proof of this empirical result.

The spin-orbit terms in the optical-model potential should exhibit effects in the differential cross section. Since the spin-flip and non-spin-flip amplitudes are incoherent, inclusion of a spin-orbit potential should tend to fill in the minima in the differential cross section predicted on the basis of a central potential (non-spin-flip) alone. Examination of Figs. 10–12 bears out this contention. It is very probable, therefore, that those cases for which the central optical model does poorly (particularly the light elements), inclusion of the spin-orbit terms will remove these difficulties. Figure 13 shows the best fit for a pure central potential for 14 Mev p on C obtained by Glassgold and Kellogg[1]; the features of Figs. 10–13 make it highly probable that this fit will be significantly improved when spin-orbit terms are included in a detailed analysis of the scattering data. The possible improvement provided by the spin-orbit potential for the light elements is not because the spin-orbit potential is a surface term, however, as has been previously conjectured since the large angle scattering amplitudes are insensitive to the shape of the spin-orbit terms (see Figs. 1 and 2).

The reaction cross section does not depend strongly on the depth of the spin-orbit term. In the approximation

method sketched above, the spin-orbit term has an effect in second order on the reaction cross section. For the case of 14 Mev p on C and a spin-orbit depth $v_S=-1$ Mev, the calculated total reaction cross section was increased over the central well value by only 0.7%.

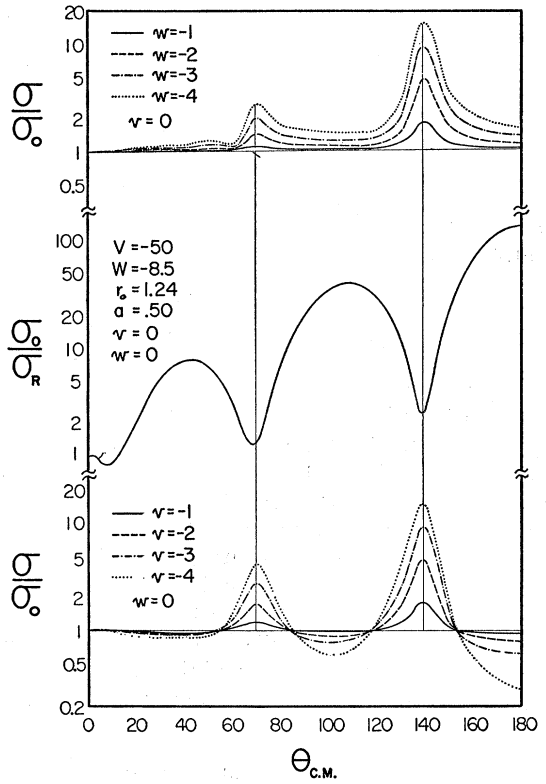

FIG. 12. The effect of the spin-orbit potential on the angular distribution of protons scattered from carbon at 14 Mev. The upper and lower sets of curves represent the differential cross section in ratio to that obtained with $v=w=0$. The middle curve is the differential cross section with $v=w=0$ in ratio to the Rutherford cross section. The effects of the incoherency between the spin-flip and non-spin-flip amplitudes is clearly demonstrated.

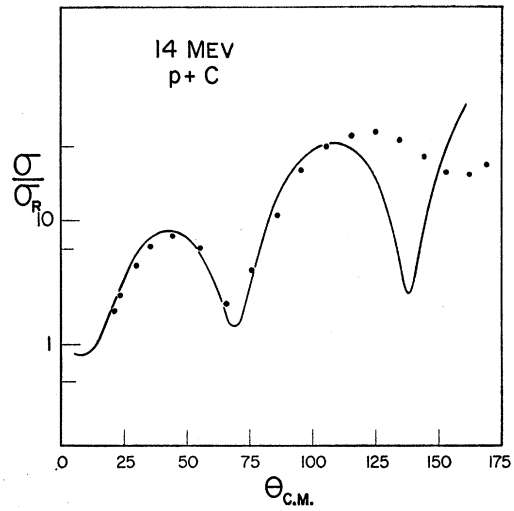

FIG. 13. The best fit to the 14-Mev p-carbon data obtained by Glassgold and Kellogg (see reference 1) with a central optical model. Comparison with Fig. 12 displays the possibility that better fits will be obtained when spin-orbit effects are included in a detailed analysis of the data.

However, a spin-orbit term may affect the reaction cross section more significantly in the following indirect manner; an entirely different best set of central parameters inferred from the analysis of the differential cross section may be obtained when the spin-orbit term is included. In particular, the depth of the imaginary part of the central well (W) may change drastically and as a consequence effect a large change in the predicted reaction cross section.

ACKNOWLEDGMENTS

The authors are particularly indebted to Dr. A. E. Glassgold for many illuminating discussions and penetrating comments. They wish to acknowledge the aid of A. Kromminga and D. Sowle in the computational aspects of this work.